Stokes' and Newton's Viscous Drag

Avi Vajpeyi
Physics Department, The College of Wooster, Wooster, Ohio 44691, USA
(Dated: May 4, 2017)

Laminar and turbulent flow regimes were studied with the help of a rotating spherical gyroscope in this experiment. We spun the gyroscope and let it slow decelerate to a halt. The deceleration occurred because of the retarding force due to the viscosity of air. By recording the frequency of rotation of the gyroscope, we were able to observe the drag force on the gyroscope to be proportionate to its angular velocity, raised to higher powers. These powers were in the range of 1-2. Stokes claimed the power to be 1 for when the region experienced laminar fluid flow. Newton on the other hand defined the power to be 2 for when the region experienced turbulent fluid flow. We determined the power to be 1.11 ± 0.12 for the case when the sphere was spun without any external resistances. This demonstrated that viscous torque experienced by the sphere with no additional resistances is best modeled by the torque equation derived from Stokes's model of viscous force for objects moving in laminar flow. In contrast, the addition of external resistances (such as paper flags) to the sphere increased the power to 2.15 ± 0.15. In this case the viscous torque is best modeled by Newton's model of viscous force for objects moving in turbulent flow. We noted that decreasing the size of the flag decreased the the power, while the orientations of the flag did not alter the power by much.

I. INTRODUCTION

The study of the flow of matter (primarily in a liquid state) known as *Rheology* began with Archimedes ($\sim$ 250 BC) [1]. Several centuries later (1687 AD), Sir Isaac Newton published his masterpiece, "Principa Mathematica" [2]. In it, Newton stated that "the resistance which arises from the lack of slipperiness originating in a fluid is proportional to the velocity by which the parts of the fluid are being separated for each other." This resistance is what we today call viscosity. In 1845 AD, after various empirical studies of the flow rate of objects in narrow tubes, Navier and Stokes created laws of motion for real fluids [1].

One of these laws was for the drag force, a law describing the resistive force against motion of a moving object in a fluid (the resistive force on motion due to a fluid's viscosity). This force is proportional to the relative velocity of the moving object and the fluid. An assumption made to derive the law was that fluid flow is laminar (the fluid flow's velocity remains constant within a given region) as seen in Figure 1. Newton on the other hand derived an equation for the drag force assuming that fluid flow is turbulent (the fluid flow's velocity varies irregularly in magnitude and direction). These two assumptions resulted with two equations for the drag force. The laminar flow assumption resulted with drag force being linearly proportional to the relative velocity of the object and fluid, while the turbulent flow assumption resulted with the drag force to be proportional to the square of the relative velocity. Experiments proved both equations to be valid for their respective fluid flow regimes (i.e. turbulent and laminar flow regimes).

One such experiment studies the effects of laminar and turbulent flow in rotational motion rather than linear motion. This can be done by spinning a sphere in a fluid and studying the rotating sphere's angular velocity and the torque acting on the sphere due to the viscous force. It is expected that at higher velocities, the torque will be proportional to the square of the angular velocity (as turbulent fluid flow is expected). Similarly, at lower velocities, the torque is expected to be directly proportional to the angular velocity (as laminar fluid flow is expected). This report discusses results from this experiment which we have replicated. We have also investigated the addition of extra resistance (in the form of rigid flags) to the sphere, and its effects on the angular velocity of the sphere.

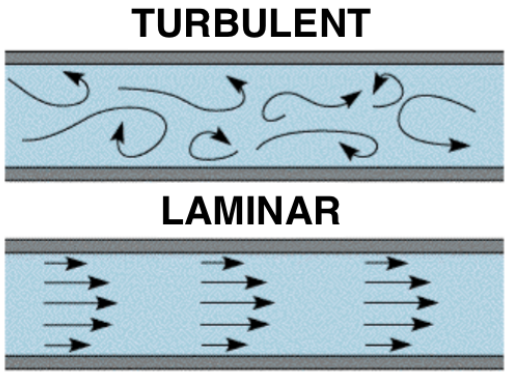

FIG. 1. The turbulent and laminar regimes of fluid flow. In laminar flow, the fluid moves more regularly than in turbulent fluid flow. This image was taken from [3].

II. THEORY

A. Viscous Drag Force

The equations for this section were obtained from [4]. To describe the viscous drag force $\vec{F}_N$, acting on a sphere of diameter d, inside a region with turbid fluid flow, we can use the following equation created by Newton

$$\vec{F}_N = \left(C_D \frac{\pi}{8} \rho d^2\right) |\vec{v}|^2 \ \hat{v}$$
$$\implies \vec{F}_N = K_2 \ |\vec{v}|^2 \ \ \hat{v} \tag{1}$$

in which C_D is the drag coefficient, ρ is the density of the fluid and $|\vec{v}| \ \hat{v}$ is the relative velocity between the fluid and the sphere. In the second line, we have combined the constants into a single constant $K_2 = -C_D \ \rho_g \ d^2\pi/8$. This gives us an equation in terms of the viscous force and velocity squared.

Now to describe the viscous drag force $\vec{F}_S$, acting on a sphere of diameter d, inside a region with laminar fluid flow, we can use the following equation created by Stokes

$$\vec{F}_S = \ (3\pi \ \eta \ d) \ |\vec{v}| \ \hat{v}$$
$$\implies \vec{F}_S = K_1 \ |\vec{v}| \ \ \hat{v} \ . \tag{2}$$

where η is the fluid dynamic viscosity or its resistance to shearing flows. Again, in the second line, we have combined the constants into a single constant $K_1 = -3\pi \ \eta \ d$. This gives us an equation in terms of the viscous force and relative velocity.

As both the $\vec{F}_S$ and $\vec{F}_N$ equations are similar, we can generalise them to

$$\vec{F} = C_n \ |\vec{v}|^n \ \hat{v} \tag{3}$$

where $n = 1, 2$ and $C_n = K_1, K_2$ for $\vec{F}_S$ and $\vec{F}_N$ respectively.

B. Viscous Drag Torque

In linear motion, net force $\vec{F}$ and mass m determine the acceleration a of an object, as described by Newton's Second Law: $\vec{F} = m \ \vec{a}$. Similarly in rotational motion, net torque $\vec{\tau}$ and moment of inertia I determine the angular acceleration $\vec{\alpha}$ of an object: $\vec{\tau} = I \ \vec{\alpha}$.

Similar to how we have a rotational analogy for Newton's second law, we have a rotational analogy for the equation for the viscous drag force in Eq. 3 and this is given by

$$\vec{\tau} = \vec{r} \times \vec{F}$$
$$= -C' \ |\vec{\alpha}|^n \ \hat{\alpha} \ ,$$

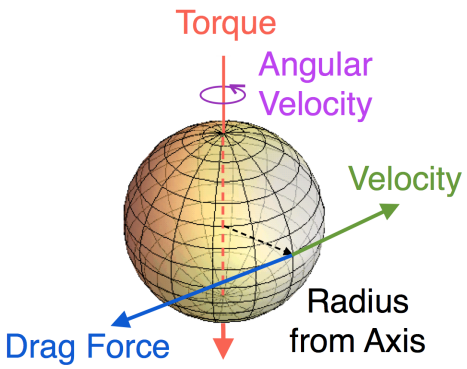

FIG. 2. Drag force on rotating sphere resulting in a drag torque.

where $C' = r \ K_n$ and $\vec{r}$ is the radius of the rotating sphere. Figure 2 shows the viscous force and the resultant torque on such a sphere.

Substituting in $\vec{\tau} = I \ \vec{\alpha}$, taking the absolute value of the equation and dividing the equation through by I, we get

$$\vec{\alpha} = -C \ |\vec{\omega}|^n \tag{4}$$
$$\implies \frac{d}{dt}\vec{\omega} = -C \ |\vec{\omega}|^n \ , \tag{5}$$

where $C = C'/I$. We can solve this differential equation for $n = 1$ and $n = 2$, and we can also take the natural logarithm of the the equation to determine the value of n.

C. Determining n

On taking the natural logarithm of Eq. 4, we get

$$\ln \alpha = \ln \left(-C\right) \ + n \ln \omega \tag{6}$$

Hence if we plot $\ln \alpha$ against $\ln \omega$, the slope of the linear fit of the data can give us n. This value can inform experimentalists if the fluid flow around the sphere is laminar or turbulent. If $n \approx 1$ then the fluid flow around the sphere is laminar as the data matches what is predicted by Eq. 2. Similarly if $n \approx 2$ then the fluid flow around the sphere is turbulent and the data matches what is predicted by Eq. 1.

D. Solving the Differential Equation

We have a separable differential equation given by Eq. 5. If we separate the dt and $d\omega$, Eq. 5 becomes

$$\frac{d\omega}{\omega^n} = -C \ dt \ . \tag{7}$$

We can now solve this equation for the two cases for n:

- **Case n = 1:** On integrating both sides of the Eq. 7 after setting $n = 1$, we get

$$\omega = \omega_0 \, e^{-C\,t} \ .$$

On taking the natural log of both sides of the equation we get

$$\ln \omega = \ln \omega_0 \ - C\,t \ . \tag{8}$$

If $\ln \omega$ is plotted against t for data that is collected for when fluid flow is laminar, the plot should result in a linear fit.

- **Case n = 2:** On integrating both sides of the Eq. 7 after setting $n = 2$, we get

$$\frac{-1}{\omega} + \frac{1}{\omega_0} = -C\,t$$
$$\implies \frac{1}{\omega} = \frac{1}{\omega_0} + C\,t \ . \tag{9}$$

If $-1/\omega$ is plotted against t for data that is collected for when fluid flow is turbulent, the plot should result in a linear fit.

In summary the solutions for the differential equation for $n = 1$ and $n = 2$ provide experimentalists with an additional way to determine if the fluid flow is laminar or turbulent. If the data collected for ω and t linearly fit Eq. 8 then we know the fluid flow is laminar. If the data linearly fits Eq. 9 then we know that the fluid flow is turbulent.

III. PROCEDURE

A. Experimental Setup

A diagram of the experimental set up used to study the fluid flow across the gyroscope can be seen in Figure 3. The gyroscope was held up by a cushion of gas and has black electrical tape along every quarter arc of its upper hemisphere. We created this cushion of gas by supplying N_2 under the gyroscope from a compressed nitrogen tank set at a constant 12 psi. This allowed us to spin the gyroscope so that the only force resisting its motion would be the drag force.

We added a laser and a light sensor as shown in Figure 3 and positioned them such that the laser bounced off the rotating gyroscope, into the light sensor. The black electrical tape that had been added does not reflect the laser. Hence when the laser is incident on the black tape, the laser will not strike the sensor. When the laser does strike the sensor, the light is read by the sensor as a peak in voltage. The voltage peak is sent to a frequency counter which counts the number of dips in the voltage (which occurs when no light reaches the sensor). The frequency counter we used was the Hewlet Packard frequency counter.

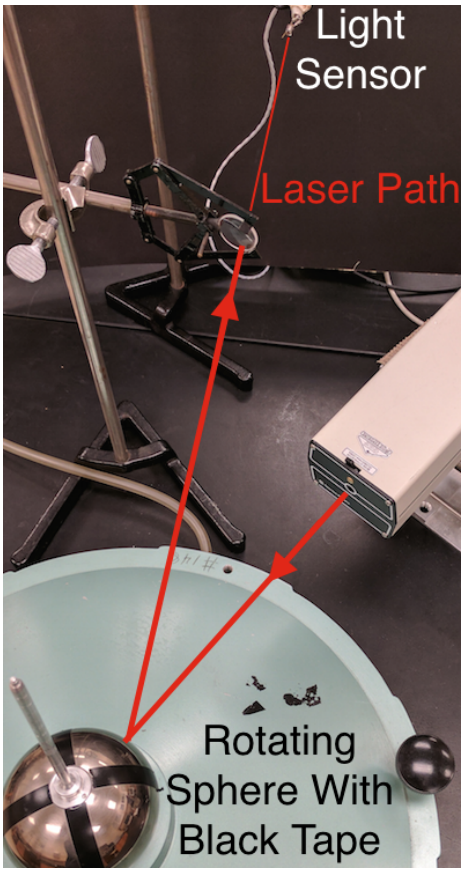

FIG. 3. Image of apparatus

The frequency counter was set to record the number of dips in voltage per second, at 10 second intervals. We called this the measured frequency. We then averaged this frequency over the 10 second interval with a LabView program. The LabView program also converted this measured frequency to the frequency of the gyroscope's rotation by dividing the measured frequency by 4 (the number of times the voltage would dip one rotation due to each strip of black tape being $\pi/2$ radians apart). A flowchart for the LabView program can be found in the appendix.

B. Data Acquisition

Once the experimental setup was ready to record the gyroscope's frequency f, we spun the gyroscope and let it remain spinning undisturbed until it stopped by itself. The force which decelerated the gyroscope was the retreading drag force due to the viscosity of air. By recording f, we were able to determine the angular velocity of the gyroscope with $\omega = 2\pi\ f$. On numerically differentiating ω (after removing outliers in the data) we were able

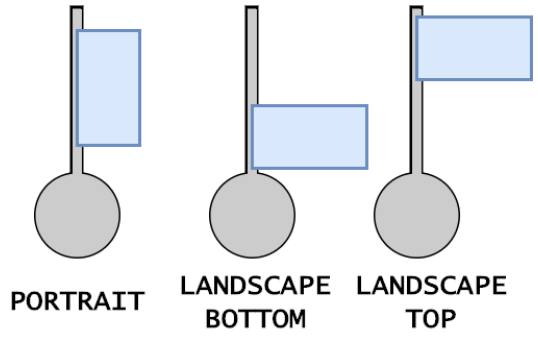

FIG. 4. A schematic to visualise the different flag orientations.

to calculate the gyroscope's angular acceleration with the central differences algorithm:

$$\alpha_n = \frac{d\omega}{dt} = \frac{\omega_{n+1} - \omega_{n-1}}{t_{n+1} - t_{n-1}} \ . \tag{10}$$

With ω and α we were able to plot ln α against ln ω as described by Eq 6 to obtain the value of n. We then repeated this experiment with the addition of multiple flags in different orientations. The different orientations of the flags can be seen in Figure 4. We even plotted the data with Eq. 8 and Eq. 9 to verify which regime of fluid flow was governing the system when different flags were attached.

IV. RESULTS AND ANALYSIS

The angular velocity ω was measured for the gyroscope without and with flags attached in different orientations as discussed in the previous section. All the flags we used were rectangular but with different areas. Flag 1 was the largest with its dimensions as 9×15 cm^2. We discovered that this flag increased the viscous torque by such a large extent that we were unable to take more than two seconds of data for this.

The next flag, Flag 2, was a smaller rectangle with dimensions 7×11 cm^2. As this flag was smaller than the previous, it did not increase the viscous torque by as large an amount as the previous flag. Hence, we were able to take data with this flag. We discovered that attaching the flag in its *portrait* orientation (see Figure 4) resulted with a smaller viscous torque than either of the *landscape* orientations. We expected this as we know that $\vec{\tau} = \vec{r} \times \vec{F}$ and with the flag oriented horizontally, the $\vec{r}$ is larger than for its vertical orientation. We were able to observe the larger torque in our data by studying the Flag 2's frequency VS time plot as seen in Figure 5. On the plot we can see that the decay of the frequency with time for the portrait orientation takes longer than for the landscape orientations. We concluded that this is due to the landscape orientations experiencing a larger torque.

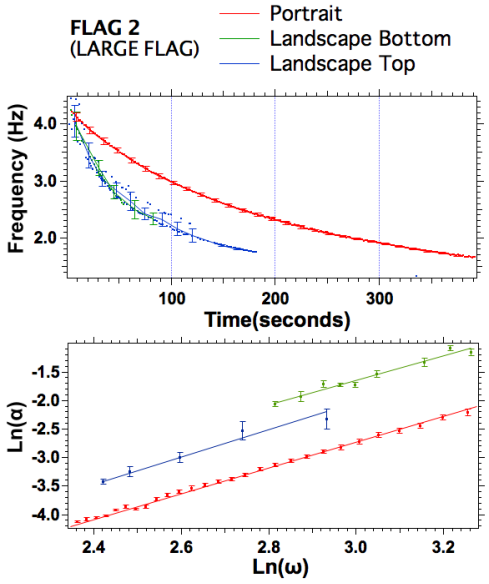

FIG. 5. Plots for Flag 2 data. The first plot is that of the frequency of revolution of the gyroscope with and the second plot is that of the natural log of angular acceleration plotted against the natural log of the angular velocity. The different colours on the graphs represent the different orientations for Flag 2.

On this plot, the dots are the data points that remained after we removed the outliers (data points with f greater/smaller than the neighbouring f by more than 0.5 Hz). The data points connected with lines are the averages of several of the dot data points neighbouring each other. We selected the number of points to average depending on how many data points were required to make the graph of the data to appear as a smooth differentiable function. This was challenging as the data fluctuated a lot and so we took several data runs with the same flag and same orientation to get smoothest data set to analyse. The uncertainty of each of the averaged f values was set to the standard deviation of the neighbouring f points that were used to calculate the average.

Using the smoothest frequency data from each experiment, we calculated the ω and then differentiated this numerically to obtain α as described in the previous section. On plotting ln α against ln ω as seen in the bottom graph of Figure 5, we were able to obtain the value of n as described in Eq. 6 from the slopes of the graphs. The uncertainty for $g(x) = \ln \alpha$ was calculated with the

TABLE I. The values of n for Eq. 6 for the different data sets. The value of n helps inform us that the gyroscope must be experiencing a net turbulent flow for the large flags and a laminar flow for the small/no flag data sets.

	Area (cm^2)	Slope (n)
FLAG 1	9×15	-
FLAG 2	7×11	
orientation 1		2.26 ± 0.06
2		2.15 ± 0.15
3		2.38 ± 0.28
FLAG 3	3.5×5.5	
orientation 1		1.25 ± 0.01
2		1.31 ± 0.02
3		1.27 ± 0.04
NO FLAG	0	1.11 ± 0.12

following equation:

$$\begin{aligned}\delta g(\omega) &= \left|\frac{d}{df}\ln\Big(-C\,\omega^n\Big)\right|\delta\omega \\ &= \frac{1}{-C\,\omega^n}\,(-C\,n\,\omega^{n-1})\,(2\pi\,\delta f) \\ &= \frac{4\pi}{\omega}\,\delta f\ .\end{aligned}$$

Here, δf is the uncertainty in the frequency of revolution of the gyroscope. Additionally, we have taken $n = 2$ in the uncertainty calculations to maximise the possible uncertainty.

The values for n that we obtained from our experiments have been recorded in Table I. From the table we can see that for Flag 2, $n \approx 2$ and for Flag 1 and no flag, $n \approx 1$. This tells us that as we increase the surface area for the flag, the turbulence increases. At smaller areas, the flag has almost laminar flow (since $n \approx 1$). For the case where there is no flag, we see that $n = 1.11 \pm 0.15$, a value which includes $n = 1$. Hence, we can see that in normal rotation of the gyroscope in air, the fluid flows around the gyroscope in a laminar fashion.

Note that for Flags 2 and 3, the values for n are only approximately near $n = 1$ and $n = 2$. This might be because the torque for which we are calculating n for may be different for different regions of the flag and gyroscope. The fluid flow may be laminar near the gyroscope, but turbulent near the flag. Hence, resulting with a value neither $n = 1$ nor $n = 2$ but inbetween.

A. Analysis with the Differential Equation Solutions

As discussed in Section II D, if the data linearly fits Eq 8, then we know that the data must have been collected from a region with laminar flow. Similarly, for data that linearly fits Eq 9, the data must have been collected in a region with turbulent fluid flow. Figure 6 contains plots for Eq 8 and Eq 9 for the data from Flags 2 and 3. From the previous section, we predicted that the Flag 2 must have been in turbulent fluid flow, while Flag 3 must have been in laminar fluid flow. The plots for Flags 2 and 3 in Figure 6 confirm this. To make our confirmation more rigorous, we took calculated the residuals of the best fit lines, in the plots for Flags 2 and 3 in Figure 6, and compared them to each other.

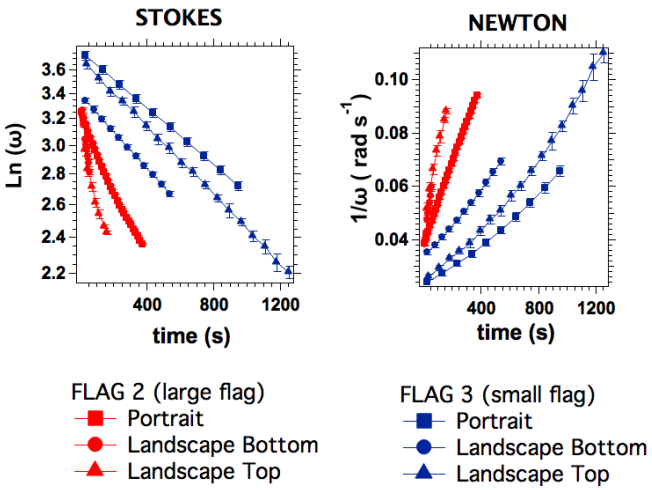

FIG. 6. Plots of the data from flags 2 and 3 to determine if the data follows the equations for viscous torque as explained in Eq. 8 and 9.

After taking weighted slopes for each of the data sets on both the plots, we created residual plots of the data as seen in Figure 7 to help us determine which of the data sets were more linear. We calculated the residual R with the following formula:

$$R = y_i - [a + b\,x_i]\ , \tag{11}$$

where the ordered pair (x_i, y_i) is the data we plotted, and a and b are the intercept and slope of the fitted line that we fitted to the plotted data. Clearly, in Figure 7 we can see that the residuals for Flag 2 are larger for when Stokes's $n = 1$ equation was used to solve the differential equation given in Eq. 5. This tells us that the data for Flag 2 varies a lot from its fit for this solution of the differential equation. Hence this tells us that the Flag 2's data is not well explained by the laminar flow's torque equation. We see instead that its residuals are smaller for Flag 2 when we use the Eq. 9 (Newton's version of the solution to the differential equation, Eq. 5), telling us that the data can be explained better by the turbulent flow's torque equation. This information can be better understood with Table II.

II has the average residuals for each data set. We have named the residuals for Flag 3 to be $R3$ and the residuals for Flag 2 to be $R2$. The difference between these will

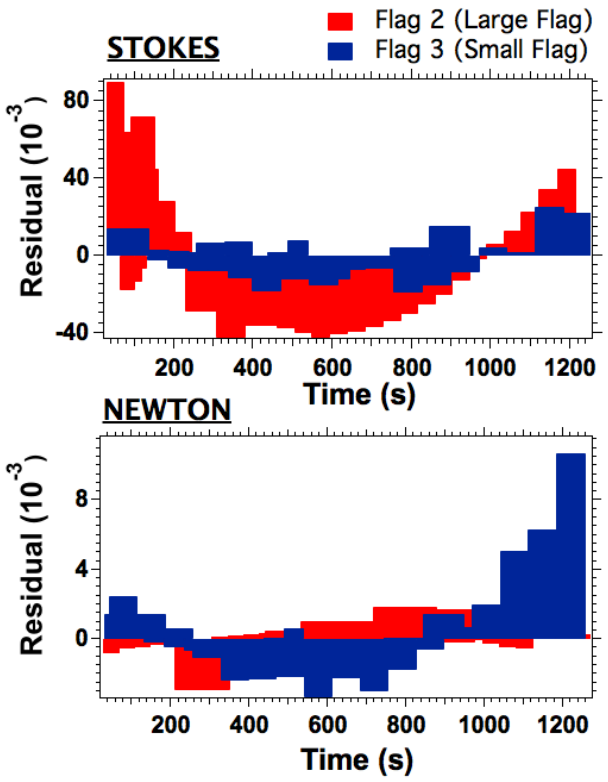

FIG. 7. Bar graphs of the residuals obtained from the linear fits of the flag 2 and 3 data as plotted in Figure 6. We can clearly see that .

TABLE II. The difference of the averaged residual values obtained from the fitted lines of the data in Figure 6 for Flags 3 and 2. R3 and R2 are average residual values from Flags 3 and 2 respectively. A full table of the data with the uncertainties can be found in the appendix.

	R3−R2	
ORIENTATION	STOKES	NEWTON
Portrait	-1.83×10^{-4}	1.12×10^{-4}
Landscape (bottom)	-2.00×10^{-3}	2.91×10^{-5}
Landscape (top)	-1.08×10^{-3}	1.08×10^{-3}

demonstrate how the linear fits of Eq. 8 better fit the Flag 3 data than Flag 2's. Similarly, the differences will also demonstrate how the fits of Eq. 9 better fit Flag 2's data than Flag 3's. As seen in the table, the first data column is for the averaged residuals for Stokes linear fits for laminar flow. We can see that $R3 - R2 < 0$, which tells us that Flag 2 has larger residuals than $R3$. Hence Flag 3 data is better fit by the Stokes model. Conversely, $R3 - R2 > 0$ for turbulent flow, implying that Flag 3 has larger residuals. This means that the Flag 2 is better fit by Newton's model.

This hence confirmed that Flag 2's data was modeled well by Newton's viscous torque equation while Flag 3's data was modeled well by Stokes' viscous torque equation.

V. CONCLUSIONS

Turbulent and laminar fluid flow are both useful physical phenomenon. Laminar flow is desirable in many situations, such as in drainage systems or airplane wings, because it is more efficient and less energy is lost. Turbulent flow can be useful for causing different fluids to mix together or for equalizing temperature. Understanding both laminar and turbulent fluid flow and their resulting drag forces hence is important. In this experiment, we studied the drag forces from laminar and turbulent fluid flow on the rotation of a sphere. We found that for a smooth gyroscope without any additional resistance, the viscous torque experienced by it is best modeled by the torque equation derived from Stokes's model of viscous force for objects moving in laminar flow. This is expected since the gyroscope is streamlined and hence air should flow around it in a steady and systematic fashion. In contrast, we noticed that with the addition of external resistance in the form of rigid flags, the viscous torque is best modeled by Newton's model of viscous force for objects moving in turbulent flow. This is expected as the addition of flags makes the structure less streamlined, and hence the air cannot move around the object as systematically as before. Additionally, we noted that altering the orientation of the flags can alter the viscous torque being experienced by the rotating body. This is because torque depends on the distance between the axis of rotation of the object and the point at which the torque is being calculated.

[1] Deepak Doraiswamy. The origins of rheology: a short historical excursion. *Rheology Bulletin*, 71(1):1–9, 2002.

[2] Isaac Newton. Principia mathematica. *Newton's principia*, page 634, 1934.

[3] Frank M White and Isla Corfield. *Viscous fluid flow*, volume 3. McGraw-Hill New York, 2006.

[4] Chang-Yu Wu. Newton's resistance law and stokes's law. `https://www.google.com/webhp?sourceid=chrome-instant&ion=1&espv=2&ie=UTF-8#q=aerosol+stokes+viscocity&*`, 2012.